Finite Control-Set Model Predictive Torque Control of Nonsinusoidal PMSM: a Generalized Approach for Torque Ripple Mitigation and MTPA Operation

Allan Gregori de Castro*, Paulo Roberto Ubaldo Guazzelli*, Stefan Thiago Cury Alves dos Santos*,
William César de Andrade Pereira†, Carlos Matheus Rodrigues de Oliveira‡,
Geyverson Teixeira de Paula § and José Roberto Boffino de Almeida Monteiro *
*São Carlos School of Engineering, Department of Electrical and Computing Engineering
University of São Paulo, São Carlos, São Paulo, Brazil
allangregori@gmail.com, paulo.ubaldo@usp.br, stefan.santos@usp.br, jrm@sc.usp.br
†WEG Drives & Controls, Jaraguá do Sul, Santa Catarina, Brazil
williamwcap@gmail.com
‡Department of Electrical Engineering
Federal University of Technology - Paraná, Apucarana, Paraná, Brazil
carlosmro@gmail.com
§School of Electrical, Mechanical and Computer Engineering
Federal University of Goiás, Goiânia, Goiás, Brazil
geyverson@gmail.com

***Abstract*—Permanent Magnet Synchronous Motors (PMSMs) may present spatial harmonics depending on the design guidelines or imprecisions on the manufacturing process. The interaction of conventional sinusoidal current feeding strategies with these spatial harmonics can produce a considerable torque ripple. This paper deals with a modified Finite Control-Set Model Predictive Torque Control (FCS-MPTC) loop as an active torque ripple minimization solution for PMSMs with spatial harmonics. The proposed approach designs a novel cost function, based on the cross product reactive instantaneous power theory. The benefits of the proposed generalized approach include providing smooth torque production and the Maximum Torque per Ampère (MTPA) operation on PMSMs with a number of spatial harmonic sources, including those on zero-sequence. The effectiveness of the presented control strategy is demonstrated comparatively to conventional sinusoidal current feeding strategy on a PMSM drive employing a three-phase four-leg two level voltage source inverter under both steady and transient state.**

***Keywords* – Finite control-set model based predictive torque control (FCS-MPTC), spatial harmonics, permanent magnet synchronous motor (PMSM), torque ripple minimization, Maximum Torque per Ampère (MTPA).**

I. Introduction

Permanent Magnet Synchronous Motors (PMSMs) are used in a wide range of applications, including household appliances [1] and vehicular traction/propulsion [2]. The motivation of their use is often associated to their higher power density and higher efficiency compared to DC or induction motors [3], [4]. Due to design guidelines or mechanical tolerances during manufacturing process, the PMSMs may suffer from spatial harmonics on PM flux linkage and stator inductances [5], [6]. Conventional control schemes which neglect the harmonic content may produce reasonable torque ripple level, which is undesirable in high-performance motion control because it is associated to the increase of vibration, speed undulation and mechanical wear and tear on mechanical drive parts, hence reducing the life of the system [7].

Mitigation of torque ripple is approached in the literature in two ways: passively and actively [8]. The former is devoted to improve the motor design. Despite its effectiveness, it may complicate the manufacturing, increase the final cost and, even if well designed, mechanical tolerances or limitations on manufacturing process still lead to torque ripple. On the other hand, the active method focuses on modifying the machine feeding strategy, such that proper harmonic stator currents circulation are intended to produce compensating harmonic torque components. As an advantage over the passive one, the active approach can be applied to existing machine drives, by improving the control algorithm and/or the drive circuitry.

The challenge of active torque ripple mitigation methods is the design and injection of proper harmonic stator currents through the stator winding.

Several approaches of active torque ripple mitigation have been presented in the literature over the last few decades. In [9] an iterative learning method is presented to update the current command based on torque transducer measurements. In [10] the required current harmonic components derives from the real-time Fourier analysis of the measurements of an accelerometer installed on machine frame. In [11] the optimal stator current is obtained from the analysis of measured speed undulations. In [12] the optimal current harmonics are designed numerically at a given operation condition based on genetic algorithm. Despite the effectiveness, these approaches

https://doi.org/10.53316/sepoc2021.024

are computationally complex since they involve iterative computations to converge to a optimized solution. The iterative process may not timely update the optimal harmonic current in transients state, not ensuring low torque ripple during torque/speed dynamics.

Alternatively to the usage of iterative solutions and additional sensors, numerous authors have reported control solutions based on the mathematical model of electromagnetic torque with the inclusion of harmonic sources. The common objective is to select the proper control variables and derive their command values to reach torque ripple minimization with minimum stator current magnitude requirement. In [13] a torque and stator flux control loop is proposed incorporating the harmonic content of non sinusoidal back electromotive force (back-EMF) on the torque and stator flux calculations. However torque ripple reduction is limited since harmonic stator flux command is not considered [14], [15]. In [15], to avoid this issue a direct torque and indirect stator flux control loop is proposed. In [16] the stator currents are selected to be controlled, and the optimized harmonic reference components are derived based on a Lagrange multiplier approach. However, the method only considers a selected range of harmonics to calculate current references and these mentioned works do not deal with inductance harmonics or zero sequence PM flux linkage harmonics. In [17] the optimal stator current command values are obtained based on Gauss-Newton procedure considering harmonics on PM flux and inductances. However only a selected set of harmonics is considered and the development does not deal with zero sequence PM flux. In [18] a geometric interpretation of optimum current design is presented including zero sequence PM flux linkage harmonics, but it is restricted to surface mounted PM machines.

Based on the exposed, the definition of novel control variables for torque ripple minimization is the primary focus of this paper to cope with the presence of harmonics on stator inductances and PM flux linkage, also benefiting the drive with those on the zero sequence. To that end, the cross product instantaneous power theory appears as a powerful tool to analyze the power flow in multi-phase circuits with nonsinusoidal voltages and currents in the time domain, and have been widely employed, for example, in the field of power conditioning with active filtering for harmonic compensation, unbalance compensation and reactive power injection [19]. Here, it is used to propose the defined active and reactive torque quantities as suitable control variables for torque ripple minimization and maximum torque per Ampère (MTPA) operation of nonsinusoidal PMSM drives, avoiding the difficulties of current or stator flux optimal harmonic reference definition.

Regardless the selected control variables, the control schemes responsible for harmonic injection require controllers with high bandwidth, and the one of conventional Proportional-Integral (PI) may not cover the critical frequencies of torque pulsations [20]. In this sense, a number of controllers have been investigated in the literature, such as sliding mode, repetitive, resonant, deadbeat and hysteresis ones [16], [20]–[23]. Recently, the Finite Control-Set Model based Predictive Control (FCS-MPC) has been extensively studied in high-performance motor drives and other systems as an interesting alternative [24]. Based on the internal model of the system, FCS-MPC predicts the future behavior of control variables and chooses as the optimal control action the feasible switching state of the power converter that minimizes a cost function designed to express the control objective, usually aiming the minimization of errors between the desirable and future predicted behavior of the controlled variables. Among the advantages, this approach provides fast dynamics of controlled variables, lesser tuning parameters and avoids modulation stage, since the control signals for power switches are directly generated by the cost function minimization process decision [24].

In this context, the goal of this paper is to combine the potentialities of the cross product instantaneous power theory and FCS-MPC to propose a modified Finite Control-Set Model Predictive Torque Control (FCS-MPTC). The proposed FCS-MPTC produces a reduced torque ripple and MTPA operation of interior mounted PMSM (IPMSM) with PM flux linkage and inductance harmonics, including those in zero sequence of $dq0$ reference space. Essentially, while conventional FCS-MPTC for PMSM extensively implements torque/flux or current control loops, in this paper it is proposed a novel cost function for torque control of IPMSM drives, built from the cross product reactive instantaneous power theory. The proposed cost function is divided in two main components. The first one is the *active torque tracking* component, responsible for active torque reference tracking and it is dominant during transient, favoring fast error mitigation. The second component is composed of three *reactive torque tracking* elements and they are responsible to lead the machine to a MTPA operation. Conceptually, this approach avoids the necessity of define harmonic current/flux references, is not limited to a finite set of selected harmonics, is not an interactive method and is suitable to various scenarios of spatial harmonics in PMSMs.

II. Machine Dynamic Model

Considering a three-phase IPMSM with Y connected stator winding, the continuous time voltage phase model in stationary abc frame is

$$\boldsymbol{v}_{abc} = R\,\boldsymbol{i}_{abc} + \boldsymbol{L}_{abc}\frac{d\,\boldsymbol{i}_{abc}}{dt} + \frac{d\,\boldsymbol{L}_{abc}}{dt}\,\boldsymbol{i}_{abc} + \omega_e\frac{d\lambda_{r,abc}}{d\theta_e} \quad (1)$$

where $\boldsymbol{v}_{abc} = [v_{an}\ v_{bn}\ v_{cn}]^T$ is the phase voltage vector with respect to the neutral point of the Y connected stator winding, $\boldsymbol{i}_{abc} = [i_a\ i_b\ i_c]^T$ is the stator phase current vector, $\lambda_{r,abc} = [\lambda_{r,a}\ \lambda_{r,b}\ \lambda_{r,c}]^T$ is the rotor permanent magnets flux linkage vector, R is the stator phase resistance, ω_e is the electrical rotor speed, θ_e is the electrical rotor position and $\boldsymbol{L}_{abc}$ is the inductance matrix, given by

$$\boldsymbol{L}_{abc} = \begin{bmatrix} L_{aa} & M_{ab} & M_{ac} \\ M_{ba} & L_{bb} & M_{bc} \\ M_{ca} & M_{cb} & L_{cc} \end{bmatrix} \quad (2)$$

where L_{aa}, L_{bb}, and L_{cc} are the self inductances and M_{ab}, M_{ba}, M_{bc}, M_{cb}, M_{ac}, and M_{ca} are the mutual inductances.

The machine model is represented in the synchronous $dq0$ reference space by the pre multiplication of (1) by the following transformation

$$\boldsymbol{T}=\sqrt{\frac{2}{3}}\begin{bmatrix}\cos(\theta_e) & \cos(\theta_e-2\pi/3) & \cos(\theta_e+2\pi/3)\\ -\sin(\theta_e) & -\sin(\theta_e-2\pi/3) & -\sin(\theta_e+2\pi/3)\\ \sqrt{2}/2 & \sqrt{2}/2 & \sqrt{2}/2\end{bmatrix}. \quad (3)$$

The application of (3) in (1) yields to

$$\boldsymbol{v}_{dq0}=R\,\boldsymbol{i}_{dq0}+\boldsymbol{L}_{dq0}\frac{d\,\boldsymbol{i}_{dq0}}{dt}+$$
$$+\,\omega_e\left(\left(\frac{d\,\boldsymbol{L}_{dq0}}{d\theta_e}+\boldsymbol{J}\,\boldsymbol{L}_{dq0}\right)\boldsymbol{i}_{dq0}+\boldsymbol{J}\,\boldsymbol{\lambda}_{r,dq0}+\frac{d\boldsymbol{\lambda}_{r,dq0}}{d\theta_e}\right) \quad (4)$$

with

$$\boldsymbol{J}=\begin{bmatrix}0 & -1 & 0\\ 1 & 0 & 0\\ 0 & 0 & 0\end{bmatrix} \quad (5)$$

and

$$\boldsymbol{L}_{dq0}=\boldsymbol{T}\boldsymbol{L}_{abc}\boldsymbol{T}^{-1}=\begin{bmatrix}L_{dd} & M_{dq} & M_{d0}\\ M_{qd} & L_{qq} & M_{q0}\\ M_{0d} & M_{0q} & L_{00}\end{bmatrix}. \quad (6)$$

The electromagnetic torque T_e produced by a IPMSM is expressed by the coenergy model as [25]

$$T_e=n_p\left(\frac{1}{2}\boldsymbol{i}_{abc}^T\frac{d\boldsymbol{L}_{abc}}{d\theta_e}\,\boldsymbol{i}_{abc}+\left(\frac{d\boldsymbol{\lambda}_{r,abc}}{d\theta_e}\right)^T\boldsymbol{i}_{abc}\right). \quad (7)$$

The application of (3) in (7) yields to

$$T_e=\boldsymbol{i}_{dq0}^T\,\boldsymbol{E}_{dq0}=\boldsymbol{i}_{dq0}\cdot\boldsymbol{E}_{dq0} \quad (8)$$

where '$\cdot$' denotes the internal product of two vectors and $\boldsymbol{E}_{dq0}=[E_d\,E_q\,E_0]^T$ is defined here as the Speed Normalized Electromechanical Voltage (SNEV), given by

$$\boldsymbol{E}_{dq0}=\;n_p\left(\frac{1}{2}\left(\frac{d\boldsymbol{L}_{dq0}}{d\theta_e}-\boldsymbol{L}_{dq0}\boldsymbol{J}+\boldsymbol{J}\boldsymbol{L}_{dq0}\right)\boldsymbol{i}_{dq0}+\right.$$
$$\left.+\,\boldsymbol{J}\boldsymbol{\lambda}_{r,dq0}+\frac{d\boldsymbol{\lambda}_{r,dq0}}{d\theta_e}\right). \quad (9)$$

III. Basics of Cross Product Instantaneous Reactive Power Theory

The cross product instantaneous power theory defines a set of instantaneous power components in the time domain based on vector relationship between voltages and currents [26]. It can be applied to multi-phase systems and no restrictions are imposed on the voltage or current waveforms, independent of the presence of harmonics or unbalances in the system. Furthermore, it is valid not only in the steady state analysis, but also in transient state [26]. Here, it is used to elucidate the control goals in proposed FCS-MPTC of nonsinusoidal IPMSM drives.

The basic definition of instantaneous active power P is almost the same in most of the power theories. It is defined as the internal product of instantaneous current and voltage vector. Thus, in the $dq0$ reference space P is calculated as

$$P=\boldsymbol{i}_{dq0}\cdot\boldsymbol{v}_{dq0}=\boldsymbol{i}_{dq0}^T\boldsymbol{v}_{dq0}=i_dv_d+i_qv_q+i_0v_0. \quad (10)$$

Based on the cross product of instantaneous current and voltage vectors, this theory defines the instantaneous vector $\boldsymbol{Q}_{dq0}$ as the reactive power vector such as[1] [26]

$$\boldsymbol{Q}_{dq0}\coloneqq\boldsymbol{i}_{dq0}\times\boldsymbol{v}_{dq0}=\begin{bmatrix}Q_{q0}\\ Q_{d0}\\ Q_{dq}\end{bmatrix}=\begin{bmatrix}i_qv_0-i_0v_q\\ i_0v_d-i_dv_0\\ i_dv_q-i_qv_d\end{bmatrix}. \quad (11)$$

Realizing that the electromagnetic torque in (8) follows the internal product definition of active power in (10), the SNEV is, thus, also source of a defined reactive torque vector $\boldsymbol{\varrho}_{dq0}=[\varrho_{q0}\,\varrho_{d0}\,\varrho_{dq}]^T$ production, given by

$$\boldsymbol{\varrho}_{dq0}=\boldsymbol{i}_{dq0}\times\boldsymbol{E}_{dq0}. \quad (12)$$

In the general concept, the reactive power is a vector perpendicular to the current and voltage ones and it does not impact the transferred active power P. Therefore, non null values of reactive torque $\boldsymbol{\varrho}_{dq0}$ are associated to an additional energy flow in the machine system that does not contribute to electromagnetic torque production. Accordingly, the minimum current required to produce active power is the one which produces null reactive power components [26]. Thus, the imposition of a real-time null reactive torque production is a consistent control goal for MTPA operation since it meets the concept of minimum current magnitude requirement for an active torque demand.

IV. Finite Control-Set Model Predictive Torque Control Implementation

The simplified structure of the proposed FCS-MPTC scheme is shown in Fig. 1. In order to allow the zero sequence current flow, a three phase four-leg two level inverter is employed and the neutral point of the Y connected stator winding is considered accessible and connected to the inverter forth leg. Regarding the control scheme, the PI speed controller provides the torque reference to the internal FCS-MPTC control loop responsible for active and reactive torque control, which is detailed in the following.

A. Converter Topology

The independent control signals S_a, S_b, S_c and S_n of the four-leg converter compose a total of 16 (2^4) feasible combinations of switching states, denoted here as $\boldsymbol{S}_f=[S_a\,S_b\,S_c\,S_n]$, with $f\in\{1,...,16\}$.

For a given $\boldsymbol{S}_f$, the phase voltages can be expressed as

$$(\boldsymbol{v}_{abc})_f=\begin{bmatrix}\boldsymbol{S}_f(1)-\boldsymbol{S}_f(4)\\ \boldsymbol{S}_f(2)-\boldsymbol{S}_f(4)\\ \boldsymbol{S}_f(3)-\boldsymbol{S}_f(4)\end{bmatrix}V_{DC} \quad (13)$$

[1]The original definition introduced in [27] is $P=\boldsymbol{v}\cdot\boldsymbol{i}$ and $Q=\boldsymbol{v}\times\boldsymbol{i}$. However this leads to a negative reactive power in inductive loads. Since $\boldsymbol{x}\times\boldsymbol{y}=-\boldsymbol{y}\times\boldsymbol{x}$ the definition is adapted to match the common concept of reactive power [26].

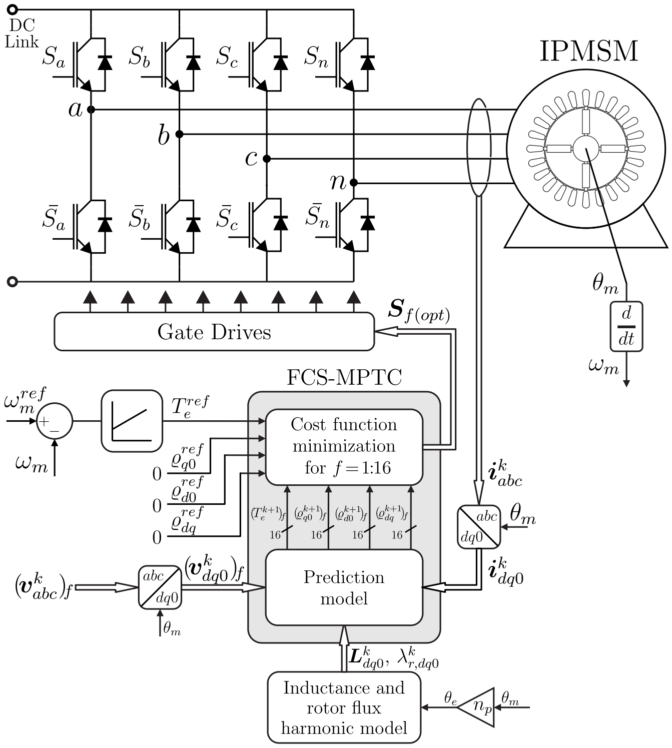

Figure 1: Control scheme of proposed FCS-MPTC.

where V_{DC} is the DC bus voltage. The application of the transformation (3) in (13) allows to obtain the stator voltage vector in $dq0$ reference space, $(\boldsymbol{v}_{dq0})_f$.

B. Prediction model

The active and reactive torque components are predicted using their discrete model. From (8) and (12), the predicted active and reactive torque to the next discrete time step are

$$T_e^{k+1} = \boldsymbol{i}_{dq0}^{k+1} \cdot \boldsymbol{E}_{dq0}^{k+1} \tag{14}$$

$$\boldsymbol{\varrho}_{dq0}^{k+1} = \boldsymbol{i}_{dq0}^{k+1} \times \boldsymbol{E}_{dq0}^{k+1}. \tag{15}$$

The future current vector value $\boldsymbol{i}_{dq0}^{k+1}$ is calculated by the discretization of (4) using the forward Euler approximation[28]. Thus, the predicted current for the (k+1)th instant considering a given stator voltage $(\boldsymbol{v}_{dq0})_f$ is

$$\begin{aligned}\boldsymbol{i}_{dq0}^{k+1} &= -R\,(\boldsymbol{L}_{dq0}^{-1})^k\,\boldsymbol{i}_{dq0}^k + (\boldsymbol{L}_{dq0}^{-1})^k\,(\boldsymbol{v}_{dq0})_f^k + \\ &- \omega_e^k\,(\boldsymbol{L}_{dq0}^{-1})^k\left(\left(\frac{d\,\boldsymbol{L}_{dq0}^k}{d\theta_e} + \boldsymbol{J}\,\boldsymbol{L}_{dq0}^k\right)\boldsymbol{i}_{dq0}^k + \right.\\ &\left. + \boldsymbol{J}\,\boldsymbol{\lambda}_{r,dq0}^k + \frac{d\boldsymbol{\lambda}_{r,dq0}^k}{d\theta_e}\right). \end{aligned} \tag{16}$$

Likewise, the future SNEV vector $\boldsymbol{E}_{dq0}^{k+1}$ is derived from (9) such that

$$\begin{aligned}\boldsymbol{E}_{dq0}^{k+1} &= n_p\left(\frac{1}{2}\left(\frac{d\boldsymbol{L}_{dq0}^{k+1}}{d\theta_e} - \boldsymbol{L}_{dq0}^{k+1}\boldsymbol{J} + \boldsymbol{J}\boldsymbol{L}_{dq0}^{k+1}\right)\boldsymbol{i}_{dq0}^{k+1} + \right.\\ &\left. + \boldsymbol{J}\boldsymbol{\lambda}_{r,dq0}^{k+1} + \frac{d\boldsymbol{\lambda}_{r,dq0}^{k+1}}{d\theta_e}\right). \end{aligned} \tag{17}$$

Assuming that inductance and rotor flux linkage are obtained from Fourier expansion or lookup tables based on rotor position measurement, i.e., $\boldsymbol{L}_{dq0}(\theta_e)$ and $\boldsymbol{\lambda}_{r,dq0}(\theta_e)$, the predicted values $\boldsymbol{L}_{dq0}^{k+1}$ and $\boldsymbol{\lambda}_{r,dq0}^{k+1}$ in (17) are obtained as follows

$$\boldsymbol{L}_{dq0}^{k+1} = \boldsymbol{L}_{dq0}(\theta_e^{k+1}) = \boldsymbol{L}_{dq0}(\theta_e^k + \omega_e^k T_s) \tag{18}$$

$$\boldsymbol{\lambda}_{r,dq0}^{k+1} = \boldsymbol{\lambda}_{r,dq0}(\theta_e^{k+1}) = \boldsymbol{\lambda}_{r,dq0}(\theta_e^k + \omega_e^k T_s), \tag{19}$$

where T_s is the sampling period. The derivative terms of inductances and rotor flux are obtained in the same manner.

C. Cost function

The proposed cost function is composed of four elements. First, the active torque error minimization is the main goal of the FCS-MPTC. Thus, this objective is written as

$$C_T = \left(T_e^{ref} - T_e^{k+1}\right)^2. \tag{20}$$

This term is dominant specially during speed reference changes when the torque error is consistent.

A secondary goal is added in the cost function to steer the machine states toward the MTPA operation. For this purpose the three reactive torque components errors are included with null reference, that is

$$C_{\varrho_{q0}} = \left(\varrho_{q0}^{k+1}\right)^2,\ C_{\varrho_{d0}} = \left(\varrho_{d0}^{k+1}\right)^2 \text{ and } C_{\varrho_{dq}} = \left(\varrho_{dq}^{k+1}\right)^2. \tag{21}$$

Finally the basis of proposed cost function is

$$C^{k+1} = c_1\,C_T + c_2\,C_{\varrho_{q0}} + c_3\,C_{\varrho_{d0}} + c_4\,C_{\varrho_{dq}}, \tag{22}$$

with c_1, c_2, c_3 and c_4 being weighting factors. The cost function (22), considering one time step horizon, is evaluated for each feasible voltage vector and the one that minimizes the cost function is chosen and then applied at the next sampling instant. In practice, digital signal processors produces one time step delay in the implementation of control actions, which can be easily compensated by pushing one discrete time step forward the cost function calculation, i.e., evaluating C^{k+2} [28].

V. Results and Discussion

In this section the simulation results are presented, illustrating the effectiveness of the proposed method in both steady and transient states, compared to conventional sinusoidal MTPA current feeding strategy method [29].

The most significant harmonic components on PM flux linkage and self/mutual inductances for the tested PMSM are detailed in Table I and II. Both parameters were obtained from Finite Element analysis considering rated stator current [30],

Table I: PM flux linkage harmonics.

	Harmonic order					
	1	3	5	7	9	11
Magnitude (mWb)	548.33	42.96	4.21	3.88	5.09	4.42
Phase(°)	2.0	6.0	9.2	-166.7	-17.8	-158.0

Table II: Self and Mutual Inductance Harmonic Components

Harmonic Order	Self Inductance		Mutual Inductance	
	Magnitude(mH)	Phase(°)	Magnitude(mH)	Phase(°)
0(DC)	31.66	0	10.75	180.0
2	11.12	-170.1	7.89	-50.2
4	1.19	-156.6	0.19	-132.6
6	0.09	28.8	0.06	88.7
8	0.23	54.2	0.05	-24.5

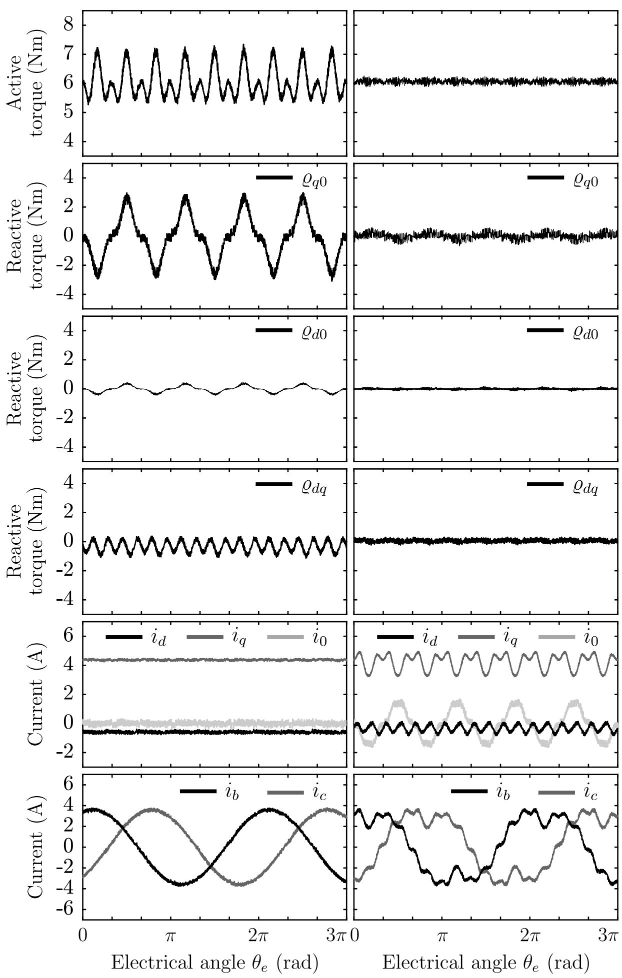

Figure 2: Steady state performance comparison. Left: sinusoidal MTPA. Right: proposed method.

[31]. The FCS-MPTC algorithm was implemented with a sampling frequency of 20kHz and the cost functions coefficients were set as $c_1 = 1$, $c_2 = 0.2$, $c_3 = 0.2$ and $c_4 = 0.2$.

Figure 2 gathers the comparison of results for conventional sinusoidal MTPA and for proposed method in steady state operation. From top to bottom, Fig. 2a shows the behavior of active torque T_e, reactive torque components ϱ_{q0}, ϱ_{d0} and

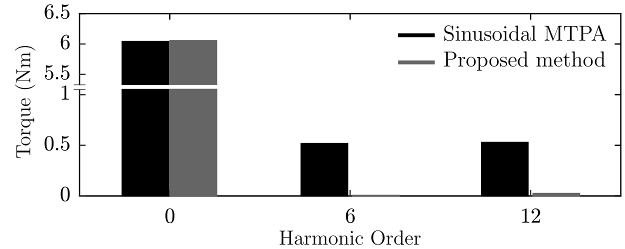

Figure 3: Comparison of harmonic distribution of torque.

ϱ_{dq}, stator current components in $dq0$ and stator phase currents i_b and i_c. Regarding the torque performance in Fig. 2, the conventional sinusoidal MTPA develops a peak to peak torque undulation with approximately 26% of the average value. These undulations are effectively reduced by the proposed method. This is reinforced by the torque harmonic distribution exhibited in Fig. 3.

In Fig. 2 it is observed that the reactive torque components are not null in conventional MTPA but varying in time with different frequencies and with non null average value in the case of ϱ_{dq}. For the proposed method, it can be seen that the reactive torques are kept closely to zero.

Fig. 4 presents a comparison of the dynamic response of the sinusoidal MTPA and the proposed method. A speed reference step is applied in $t = 0,1$ s and a 5 Nm load disturbance step in $t = 0.8$ s. From top to bottom, Fig. 4 shows the results of rotor speed ω_m, active estimated torque T_e, reactive estimated torque ϱ_{q0}, reactive estimated torque ϱ_{d0}, reactive estimated torque ϱ_{dq}, $dq0$ stator currents and abc stator currents.

Despite the fact that FCS-MPTC inherently takes into account the plant model with its coupling terms, during the torque variations the cost due to the torque error is dominant compared to the reactive torque error components. Thus, the control might not track exactly the MTPA trajectory, with exact decoupled dynamics, during transients but focuses on fast torque error mitigation. In both cases a quite similar torque dynamic is observed and, therefore, it can be concluded that the proposed FCS-MPTC method is also capable to mitigate torque undulations during transients without deterioration of the dynamic performance.

VI. CONCLUSION

This paper proposes a modified FCS-MPTC for nonsinusoidal PMSM drives aiming torque ripple reduction and maximum torque per Ampère. The novelty relies on the analysis of torque model using the cross product instantaneous power theory to build a novel cost function, addressing null electromagnetic torque ripple with MTPA operation in machines with spatial harmonics on inductances and PM flux linkage, including the zero sequence quantities participation. Hence, the proposed approach do not mitigate zero sequence current circulation, instead, it considers its contribution in favor of electromagnetic torque production.

By selecting the active and reactive torque components as control variables, the complexity of defining harmonic current or stator flux references is avoided. While the active torque command comes from and outer control loop, the reactive torque references are null to meet MTPA.

The proposed cost function of FCS-MPTC possesses a generalized formulation, not limited to selected harmonics. This generalized feature allows the simple particularization to other synchronous machine topologies, for which the reactive torque components in the cost function meet conventional control goals discussed in earlier works [15], [18], [29].

The results show that the pulsating torque is indeed suppressed by the proposed FCS-MPTC and the MPTA tracking is obtained since reactive power components are kept closely to zero.

In further work it is aimed the investigation of proposed approach in cases with machine asymmetries such as unbalanced phase back-EMFs or open phase fault condition that also leads to torque pulsations.

ACKNOWLEDGMENT

The authors would like to thank the financial support granted by National Council of Research and Development (CNPq), Coordenação de Aperfeiçoamento de Pessoal de Nível Superior - Brasil (CAPES) - Finance Code 001, Goiás Research Foundation (FAPEG), and São Paulo Research Foundation (FAPESP), grant #2006/04226-0.

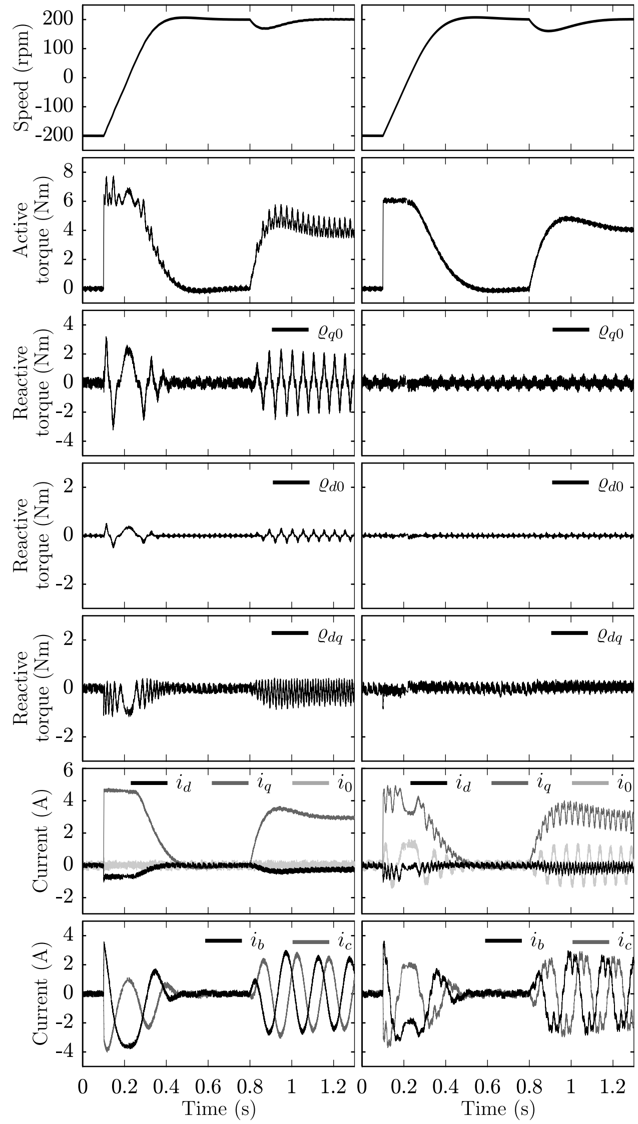

Figure 4: Dynamic response comparison. Left: sinusoidal MTPA. Right: proposed method.

REFERENCES

[1] D.-K. Kim, K.-W. Lee, and B.-I. Kwon, "Commutation Torque Ripple Reduction in a Position Sensorless Brushless DC Motor Drive," *IEEE Trans. Power Electron.*, vol. 21, no. 6, pp. 1762–1768, nov 2006.

[2] A. Boglietti, A. M. El-Refaie, O. Drubel, A. M. Omekanda, N. Bianchi, E. B. Agamloh, M. Popescu, A. Di Gerlando, and J. Borg Bartolo, "Electrical Machine Topologies: Hottest Topics in the Electrical Machine Research Community," *IEEE Ind. Electron. Mag.*, vol. 8, no. 2, pp. 18–30, jun 2014.

[3] M. Melfi, S. Evon, and R. McElveen, "Induction versus permanent magnet motors," *IEEE Ind. Appl. Mag.*, vol. 15, no. 6, pp. 28–35, nov 2009.

[4] T. J. E. Miller, *Brushless permanent-magnet and reluctance motor drives*. Oxford: Clarendon Press, 1993.

[5] H. Dhulipati, S. Mukundan, C. Lai, K. Mukherjee, J. Tjong, and N. C. Kar, "Multiple Reference Frame-Based Extended Concentrated Wound PMSM Model Considering PM Flux Linkage and Inductance Harmonics," *IEEE Trans. Energy Convers.*, vol. 34, no. 2, pp. 731–740, jun 2019.

[6] K. Wang, Z. Q. Zhu, G. Ombach, and W. Chlebosz, "Average Torque Improvement of Interior Permanent-Magnet Machine Using Third Harmonic in Rotor Shape," *IEEE Trans. Ind. Electron.*, vol. 61, no. 9, pp. 5047–5057, sep 2014.

[7] Z. Q. Zhu and J. H. Leong, "Analysis and mitigation of torsional vibration of PM brushless AC/DC drives with direct torque controller," *IEEE Trans. Ind. Appl.*, vol. 48, no. 4, pp. 1296–1306, 2012.

[8] T. Jahns and W. Soong, "Pulsating torque minimization techniques for permanent magnet AC motor drives-a review," *IEEE Trans. Ind. Electron.*, vol. 43, no. 2, pp. 321–330, apr 1996.

[9] W. Qian, S. Panda, and J.-X. Xu, "Torque Ripple Minimization in PM Synchronous Motors Using Iterative Learning Control," *IEEE Trans. Power Electron.*, vol. 19, no. 2, pp. 272–279, mar 2004.

[10] Tinghsu Su, S. Hattori, M. Ishida, and T. Hori, "Suppression control method for torque vibration of AC motor utilizing repetitive controller with Fourier transform," *IEEE Trans. Ind. Appl.*, vol. 38, no. 5, pp. 1316–1325, sep 2002.

[11] G. Feng, C. Lai, J. Tian, and N. C. Kar, "Multiple Reference Frame Based Torque Ripple Minimization for PMSM Drive under Both Steady-State and Transient Conditions," *IEEE Trans. Power Electron.*, vol. 34, no. 7, pp. 6685–6696, 2019.

[12] C. Lai, G. Feng, K. Lakshmi Varaha Iyer, K. Mukherjee, and N. C. Kar, "Genetic Algorithm-Based Current Optimization for Torque Ripple Reduction of Interior PMSMs," *IEEE Trans. Ind. Appl.*, vol. 53, no. 5, pp. 4493–4503, 2017.

[13] A. H. Abosh, Z. Q. Zhu, and Y. Ren, "Reduction of torque and flux ripples in space vector modulation-based direct torque control of asymmetric permanent magnet synchronous machine," *IEEE Trans. Power Electron.*, vol. 32, no. 4, pp. 2976–2986, 2017.

[14] L. Zhong, M. Rahman, W. Hu, and K. Lim, "Analysis of direct torque control in permanent magnet synchronous motor drives," *IEEE Trans. Power Electron.*, vol. 12, no. 3, pp. 528–536, may 1997.

[15] S. B. Ozturk and H. A. Toliyat, "Direct Torque and Indirect Flux Control of Brushless DC Motor," *IEEE/ASME Trans. Mechatronics*, vol. 16, no. 2, pp. 351–360, apr 2011.

[16] G. Feng, C. Lai, and N. C. Kar, "An Analytical Solution to Optimal Stator Current Design for PMSM Torque Ripple Minimization With Minimal Machine Losses," *IEEE Trans. Ind. Electron.*, vol. 64, no. 10, pp. 7655–7665, oct 2017.

[17] A. Madani, J. P. Barbot, F. Colamartino, and C. Marchand, "Reduction of torque pulsations by inductance harmonics identification of a permanent-magnet synchronous machine," *IEEE Conf. Control Appl. - Proc.*, no. 1,

pp. 787–792, 1995.
[18] D. Flieller, N. K. Nguyen, P. Wira, G. Sturtzer, D. O. Abdeslam, and J. Merckle, "A Self-Learning Solution for Torque Ripple Reduction for Nonsinusoidal Permanent-Magnet Motor Drives Based on Artificial Neural Networks," *IEEE Trans. Ind. Electron.*, vol. 61, no. 2, pp. 655–666, feb 2014.
[19] F. Harirchi and M. G. Simoes, "Enhanced Instantaneous Power Theory Decomposition for Power Quality Smart Converter Applications," *IEEE Trans. Power Electron.*, vol. 8993, no. 99, pp. 1–15, 2018.
[20] L. Springob and J. Holtz, "High-bandwidth current control for torque-ripple compensation in PM synchronous machines," *IEEE Trans. Ind. Electron.*, vol. 45, no. 5, pp. 713–721, 1998.
[21] P. Mattavelli, L. Tubiana, and M. Zigliotto, "Torque-Ripple Reduction in PM Synchronous Motor Drives Using Repetitive Current Control," *IEEE Trans. Power Electron.*, vol. 20, no. 6, pp. 1423–1431, nov 2005.
[22] S. J. Park, H. W. Park, M. H. Lee, and F. Harashima, "A new approach for minimum-torque-ripple maximum-efficiency control of BLDC motor," *IEEE Trans. Ind. Electron.*, vol. 47, no. 1, pp. 109–114, 2000.
[23] J. Liu, H. Li, and Y. Deng, "Torque Ripple Minimization of PMSM Based on Robust ILC Via Adaptive Sliding Mode Control," *IEEE Trans. Power Electron.*, vol. 33, no. 4, pp. 3655–3671, 2018.
[24] S. Kouro, P. Cortes, R. Vargas, U. Ammann, and J. Rodriguez, "Model Predictive Control—A Simple and Powerful Method to Control Power Converters," *IEEE Trans. Ind. Electron.*, vol. 56, no. 6, pp. 1826–1838, jun 2009.
[25] N. Nakao and K. Akatsu, "Suppressing pulsating torques: Torque ripple control for synchronous motors," *IEEE Ind. Appl. Mag.*, vol. 20, no. 6, pp. 33–44, 2014.
[26] H. Akagi, E. H. Watanabe, and M. Aredes, "The Instantaneous Power Theory," in *Instant. Power Theory Appl. to Power Cond.* Hoboken, NJ, USA: John Wiley & Sons, Inc., 2007, pp. 41–107.
[27] S. Togasawa, T. Murase, H. Nakano, and A. Nabae, "Reactive Power Compensation based on An Novel Cross Vector Theory." *IEEJ Trans. Ind. Appl.*, vol. 114, no. 3, pp. 340–341, 1994.
[28] P. Cortes, J. Rodriguez, C. Silva, and A. Flores, "Delay compensation in model predictive current control of a three-phase inverter," *IEEE Trans. Ind. Electron.*, vol. 59, no. 2, pp. 1323–1325, 2012.
[29] M. Preindl and S. Bolognani, "Model Predictive Direct Torque Control With Finite Control Set for PMSM Drive Systems, Part 1: Maximum Torque Per Ampere Operation," *IEEE Trans. Ind. Informatics*, vol. 9, no. 4, pp. 1912–1921, 2013.
[30] G. T. De Paula, J. R. B. De Monteiro, B. P. De Alvarenga, T. E. De Almeida, W. C. Pereira, and M. P. De Santana, "On-Load Back EMF of PMSM Using Maxwell Stress Tensor," *IEEE Trans. Magn.*, vol. 54, no. 7, 2018.
[31] C. Filho, B. P. De Alvarenga, and G. T. De Paula, "On-Load Apparent Inductance Derivative of IPMSM: Assessment Method and Torque Estimation," *IEEE Trans. Magn.*, vol. 56, no. 4, 2020.